Synthesis and Characterization of Te_2SeO_7: A Powder Second-Harmonic-Generating Study of TeO_2, Te_2SeO_7, Te_2O_5, and $TeSeO_4$

Yetta Porter, Kang Min Ok, N. S. P. Bhuvanesh, and P. Shiv Halasyamani*

Department of Chemistry, University of Houston, 4800 Calhoun Boulevard, Houston, Texas 77204-5641

Received December 21, 2000. Revised Manuscript Received March 20, 2001

The synthesis and characterization of a noncentrosymmetric tellurium selenate, Te_2SeO_7, is reported. In addition, the powder second-harmonic-generating (SHG) properties of TeO_2, Te_2SeO_7, Te_2O_5, and $TeSeO_4$ have been measured, using 1064 nm radiation. Through the powder SHG experiments, we are able to determine that TeO_2 is not phase-matchable, whereas Te_2SeO_7, Te_2O_5, and $TeSeO_4$ are phase-matchable. Also, TeO_2, Te_2SeO_7, Te_2O_5, and $TeSeO_4$ have SHG efficiencies of 5, 200, 400, and 400 times SiO_2, respectively. The relative SHG efficiencies may be understood by examining the structure of each material. Through the powder SHG measurements, we estimate the average nonlinear optical bond susceptibility, $\langle d^{2\omega}_{ijk} \rangle$, for each material.

Introduction

One of the continuing challenges in materials chemistry concerns the elucidation of structure−property relationships. This is especially true with second-order nonlinear optical (NLO), i.e., second-harmonic-generating (SHG), materials.[1−5] Viable SHG materials must possess the following attributes: transparency in the relevant wavelengths, ability to withstand laser irradiation, and chemical stability. Most importantly, the material in question must be crystallographically noncentrosymmetric (NCS). Mathematically, it has been known for some time that only a NCS arrangement of atoms may produce a second-order NLO response.[6] Thus, to understand SHG from a materials standpoint, it is important to understand the chemical and structural implications of NCS. We recently reviewed the known NCS oxides[3] and determined that cations susceptible to a second-order Jahn−Teller (SOJT) distortion were found in nearly half, ∼45%, of these materials. A SOJT distortion[7−13] is concerned with structural changes attributable to a nondegenerate ground state interacting with a low-lying excited state. The distortion occurs when the energy gap between the highest occupied (HOMO) and lowest unoccupied (LUMO) molecular orbitals is small *and* there is a symmetry-allowed distortion permitting the mixing of the HOMO and LUMO states. With oxides, two families of metals can undergo SOJT distortions: octahedrally coordinated d^0 transition metals and cations with nonbonded electron pairs. With the former, the mixing of HOMO and LUMO is always symmetry-allowed, with the energy between the orbitals correlated with the size and charge of the cation.[7−13] With the latter, the stereoactive lone pair is attributable to the mixing between the s and p orbitals of the metal and oxygen atoms, respectively. An example using Sb^{3+} is illustrative. Four-coordinate antimony might be expected to have tetrahedral symmetry (T_d). However, in this geometry the s^2 electron pair would occupy a strongly antibonding a_1* orbital (HOMO). As such, a distortion occurs to square-pyramidal geometry (C_{4v}) that lowers the energy of the HOMO s orbital by mixing it with the LUMO p orbital, i.e., s−p mixing. Thus, the HOMO is stabilized, and the lone pair becomes stereochemically active, resulting in the asymmetric coordination environment.

We suggest that one manner in which to increase the incidence of NCS is to synthesize oxides that contain cations susceptible to SOJT distortions. We also suggest that the SOJT distortions observed in these materials will not only alter the symmetry from centrosymmetric to NCS but also will occur in a cooperative manner. This cooperative distortion will polarize the M−O bonds, resulting in a large SHG response. Specifically, we have been investigating the synthesis of oxides that contain cations with nonbonded electron pairs.[14−16] Recently, we reported the synthesis and NLO behavior of $TeSeO_4$ that

(1) Keszler, D. A. *Curr. Opin. Solid State Mater. Sci.* **1999**, *4*, 155.
(2) Becker, P. *Adv. Mater.* **1998**, *10*, 979.
(3) Halasyamani, P. S.; Poeppelmeier, K. R. *Chem. Mater.* **1998**, *10*, 2753.
(4) Marder, S. R.; Sohn, J. E.; Stucky, G. D. *Materials for Non-Linear Optics*: *Chemical Perspectives*; American Chemical Society: Washington, DC, 1991.
(5) Chen, C.; Liu, G. *Annu. Rev. Mater. Sci.* **1986**, *16*, 203.
(6) Nye, J. F. *Physical Properties of Crystals*; Oxford University Press: Oxford, U.K., 1957.
(7) Opik, U.; Pryce, M. H. L. *Proc. R. Soc. London* **1957**, *A238*, 425.
(8) Bader, R. F. W. *Mol. Phys.* **1960**, *3*, 137.
(9) Bader, R. F. W. *Can. J. Chem.* **1962**, *40*, 1164.
(10) Pearson, R. G. *J. Am. Chem. Soc.* **1969**, *91*, 4947.
(11) Pearson, R. G. *J. Mol. Struct. (THEOCHEM)* **1983**, *103*, 25.
(12) Wheeler, R. A.; Whangbo, M.-H.; Hughbanks, T.; Hoffmann, R.; Burdett, J. K.; Albright, T. A. *J. Am. Chem. Soc.* **1986**, *108*, 2222.
(13) Kunz, M.; Brown, I. D. *J. Solid State Chem.* **1995**, *115*, 395.
(14) Halasyamani, P. S.; O'Hare, D. *Chem. Mater.* **1997**, *10*, 6646.
(15) Halasyamani, P. S.; O'Hare, D. *Inorg. Chem.* **1997**, *36*, 6409.
(16) Porter, Y.; Bhuvanesh, N. S. P.; Halasyamani, P. S. *Inorg. Chem.* **2001**, *40*, 1172.

10.1021/cm001414u CCC: $20.00
Published on Web 05/04/2001

has a SHG efficiency of 400 times quartz.[16] In this paper we report the synthesis, characterization, and SHG behavior of Te_2SeO_7. In addition, we compare the powder SHG behavior of TeO_2, Te_2SeO_7, Te_2O_5, and $TeSeO_4$ and discuss their structure−property relationships, as well as approximate their NLO susceptibilities.

Experimental Section

Synthesis. Caution! Use appropriate safety measures to avoid toxic SeO_2 and TeO_2 dust contamination.

TeO_2 (Aldrich, 99%) was used as received.

Te_2SeO_7 was synthesized by combining TeO_2 (0.500 g, 3.13×10^{-3} mol) with H_2SeO_4 (Aldrich; a 40 wt % solution, 2.20 mL, 8.54×10^{-3} mol) in a large test tube. The mixture was stirred and heated in an oil bath to 160 °C for 4 h. The resultant white powder was washed with water, to remove excess H_2SeO_4, and dried.

Te_2O_5 was synthesized by combining TeO_2 (Aldrich; 99%) and $TeO_3{\cdot}H_2O$. $TeO_3{\cdot}H_2O$ was obtained by heating $Te(OH)_6$ (Aldrich) at 200 °C overnight. The resultant yellow powder is amorphous to X-rays and is assumed to be $TeO_3{\cdot}H_2O$ based on H_2O loss during the dehydration. If $Te(OH)_6$ is fully dehydrated to TeO_3 and subsequently reacted with TeO_2, a mixture of Te_2O_5 and Te_4O_9 is formed. $TeO_3{\cdot}H_2O$ (0.576 g, 2.98×10^{-3} mol) was combined with TeO_2 (0.476 g, 2.98×10^{-3} mol), pressed into a pellet, and placed in a quartz tube that was subsequently evacuated and sealed. The tube was held at 400 °C for 24 h and cooled at a rate of 2 °C min^{-1} to room temperature. The resultant pale yellow powder was found to be a mixture of Te_2O_5 and TeO_2 by powder XRD. TeO_2 was removed by washing the powder with 1 M HCl. The XRD pattern of the purified powder was shown to be in excellent agreement with that reported for Te_2O_5.

$TeSeO_4$ was synthesized as previously reported.[16]

Powder Diffraction. Powder XRD data for TeO_2, Te_2SeO_7, Te_2O_5, and $TeSeO_4$ were recorded on a SCINTAG XDS2000 automated diffractometer at room temperature (Cu Kα radiation, $\theta-\theta$ mode, flat-plate geometry).

Infrared Measurements. Infrared spectra for Te_2SeO_7 were recorded on a Matteson FTIR 5000 spectrometer in the 400−4000 cm^{-1} range, with the sample pressed between two KBr pellets. IR (cm^{-1}): ν(Se−O) 1162, 1131, 919, 876, 840, 800; ν(Te−O) 775, 649; ν(Te−O−Te) 510, 435. The assignments are in good agreement with those reported earlier.[17]

Second-Order NLO Measurements. Powder SHG measurements were performed on a modified Kurtz-NLO[18] system using 1064 nm light. A Continuum Minilite II laser, operating at 15 Hz, was used for all measurements. Because the SHG efficiency of powders has been shown to depend strongly on the particle size,[19] polycrystalline TeO_2, Te_2SeO_7, Te_2O_5, and $TeSeO_4$ were ground separately and sieved (Newark Wire Cloth Co.) into distinct particle size ranges, <20, 20−45, 45−63, 63−75, 75−90, and 90−125 μm. To make relevant comparisons with known SHG materials, crystalline SiO_2 and $LiNbO_3$ were also ground and sieved into the same particle size ranges. All of the powders were placed in separate capillary tubes. No index-matching fluid was used in any of the experiments. The SHG light, i.e., 532 nm green light, was collected in reflection and detected by a photomultiplier tube (Oriel Instruments). To detect only the SHG light, a 532 nm narrow band-pass interference filter was attached to the tube. A digital oscilloscope (Tektronix TDS 3032) was used to view the SHG signal. For all of the measurements, $I^{2\omega}/I^{2\omega}$ (SiO_2) is taken for a particle size range from 45 to 63 μm.

Results

Structures of TeO_2, Te_2SeO_7, Te_2O_5, and $TeSeO_4$. The structure of TeO_2 has been known for some time,[20] so only a brief description will be given here. TeO_2 crystallizes in the tetragonal space group $P4_12_12$ (No. 92) and has a three-dimensional structure consisting of corner-shared $[TeO_{4/2}]^0$ polyhedra. The Te^{4+} cations are in an asymmetric coordination environment owing to the stereoactive lone pair.

Table 1. Powder XRD Data for Te_2SeO_7 [Refined Unit Cell of a = 4.8042(7) Å, b = 8.623(1) Å, and c = 7.354(3) Å and Space Group of $Pmn2_1$ (No. 31)]

h	k	l	d_{obs}	d_{calc}	I_{obs}	I_{calc}[a]
0	1	0	7.361	7.355	41	35
1	1	0	5.600	5.596	76	75
2	0	0	4.309	4.312	21	17
1	0	1	4.199	4.197	44	47
0	1	1	4.021	4.022	100	100
2	1	0	3.720	3.720	79	68
0	2	0	3.679	3.677	9	9
1	1	1	3.646	3.645	55	55
1	2	0	3.382	3.383	44	42
2	1	1	2.940	2.941	61	63
0	2	1	2.920	2.920	70	76
2	2	0	2.799	2.798	27	28
1	2	1	2.766	2.766	20	22
3	0	1	2.465	2.467	49	44
0	3	0	2.452	2.452	92	91
2	2	1	2.418	2.418	23	26
0	0	2	2.403	2.402	15	18
1	3	0	2.359	2.358	71	65
3	1	1	2.338	2.339	10	7
0	1	2	2.283	2.283	3	3
3	2	0	2.266	2.265	12	10
1	1	2	2.207	2.207	2	2
0	3	1	2.183	2.184	10	11
4	0	0	2.156	2.156	10	8
2	3	0	2.131	2.131	27	27
1	3	1	2.117	2.117	5	4
2	0	2	2.097	2.098	6	6
3	2	1	2.048	2.048	3	3
2	1	2	2.018	2.018	18	21
1	2	2	1.959	1.959	4	3
4	1	1	1.900	1.900	4	2
3	3	0	1.865	1.865	2	1
2	2	2	1.822	1.823	15	13
1	4	0	1.799	1.798	15	17
3	1	2	1.788	1.788	10	10
3	3	1	1.739	1.739	30	31
4	2	1	1.735	1.734	5	5
0	3	2	1.716	1.716	18	19
2	4	0	1.691	1.691	7	10
5	1	0	1.679	1.679	10	8
3	2	2	1.648	1.648	14	14
5	1	1	1.586	1.585	12	11
0	1	3	1.565	1.565	7	6
5	2	0	1.562	1.561	5	4
3	4	0	1.549	1.549	5	4

[a] Calculated using the atomic coordinates for Te_2SO_7[21−23] but substituting selenium for sulfur.

Te_2SeO_7 is isostructural with Te_2SO_7 and crystallizes in the orthorhombic space group $Pmn2_1$ (No. 31).[21−23] The unit cell, space group, d_{obs}, d_{calc}, I_{obs}, and I_{calc} are given in Table 1. Briefly, Te_2SeO_7 has a two-dimensional crystal structure consisting of $Se^{6+}O_4$ tetrahedra that are linked to distorted $Te^{4+}O_4$ groups (see Figure 1a,b). Each selenium atom is in a regular tetrahedral environment, bonded to four oxygen atoms, whereas each tellurium, although also bonded to four oxygen atoms,

(17) Gaitan, M.; Jerez, A.; Pico, C.; Veiga, M. L. *Mater. Res. Bull.* **1985**, *20*, 1069.
(18) Kurtz, S. K.; Perry, T. T. *J. Appl. Phys.* **1968**, *39*, 3798.
(19) Dougherty, J. P.; Kurtz, S. K. *J. Appl. Crystallogr.* **1976**, *9*, 145.
(20) Leciejewicz, J. *Z. Kristallogr.* **1961**, *116*, 345.
(21) Mayer, H.; Pupp, G. *Monash. Chem.* **1976**, *107*, 721.
(22) Johansson, G. B.; Lindqvist, O. *Acta Crystallogr.* **1976**, *B32*, 2720.
(23) Loub, J.; Podlahova, J.; Novak, C. *Acta Crystallogr.* **1976**, *B32*, 3115.

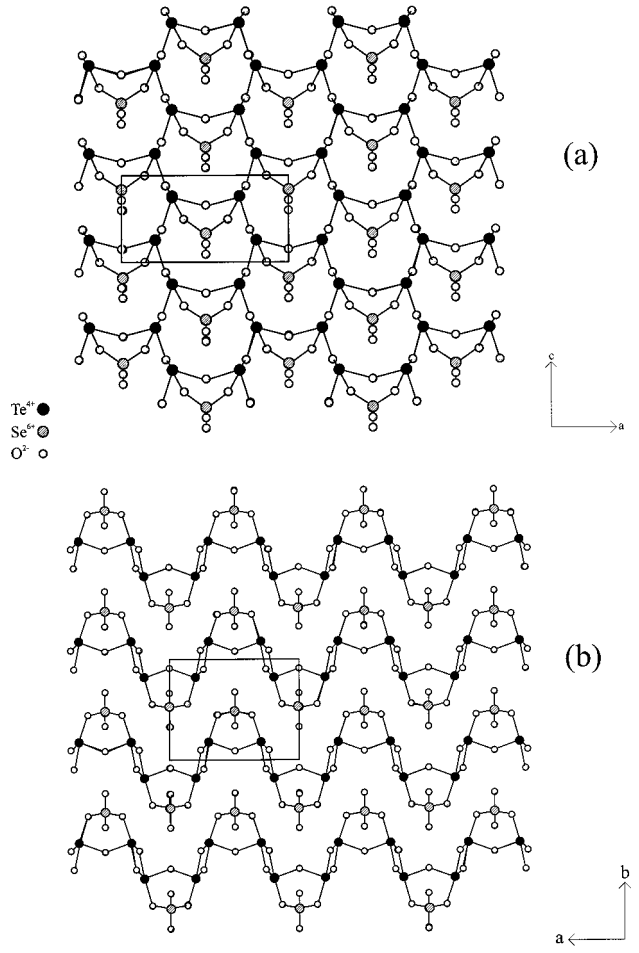

Figure 1. Ball-and-stick representation of Te_2SeO_7 along the (a) [0, 1, 0] and (b) [0, 0, 1] directions. Note that atomic coordinates and symmetry information were taken from Te_2SO_7.[21−23]

is in an asymmetric coordination environment owing to the nonbonded electron pair. In connectivity terms, the SeO_4 and TeO_4 groups can be formulated as $[SeO_{2/2}O_{2/1}]^0$ and $[TeO_{4/2}]^0$ moieties. The $[SeO_{2/2}O_{2/1}]^0$ and $[TeO_{4/2}]^0$ groups link, forming sheets in the *ac* plane (see Figure 1a). The sheets are built of "rings" of six corner-shared TeO_4 groups. Within each of these rings are the SeO_4 tetrahedra that either point up, along the [0, 0, 1] direction, or down, along the [0, 0, −1] direction. The alternating SeO_4 tetrahedra pucker these sheets along the [0, 1, 0] and [0, −1, 0] directions (see Figure 1b). As seen in Figure 1b, the intersheet interactions are dominated by both the SeO_4 tetrahedra and the TeO_4 groups.

Lindqvist and Moret reported Te_2O_5,[24] which crystallizes in the monoclinic space group $P2_1$ (No. 4). The material consists of an ordered array of Te^{4+} and Te^{6+} cations that are connected to four and six oxygen atoms, respectively. With regards to connectivity, the TeO_4 and TeO_6 groups can be formulated as $[TeO_{4/2}]^0$ and $[TeO_{6/2}]^0$ polyhedra. Te^{4+} is in an asymmetric coordination environment attributable to the stereoactive lone pair, whereas Te^{6+} is in a nearly regular octahedral environment.

The synthesis and crystal structure of $TeSeO_4$ [monoclinic, space group *Ia* (No. 9)] have recently been published.[16] Briefly, the structure consists of $[TeO_{5/2}]^-$ anions that are linked to $[SeO_{3/2}]^+$ cations. Both the Te^{4+} and Se^{4+} cations are in distorted environments owing to their lone pair.

(24) Lindqvist, O.; Moret, J. *Acta Crystallogr.* **1973**, *B29*, 643.

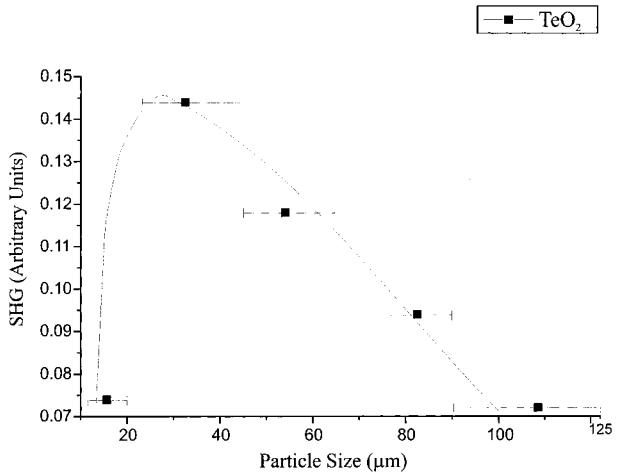

Figure 2. Phase-matching curve, i.e., particle size vs SHG intensity, for TeO_2. The curve drawn is to guide the eye and is not a fit to the data.

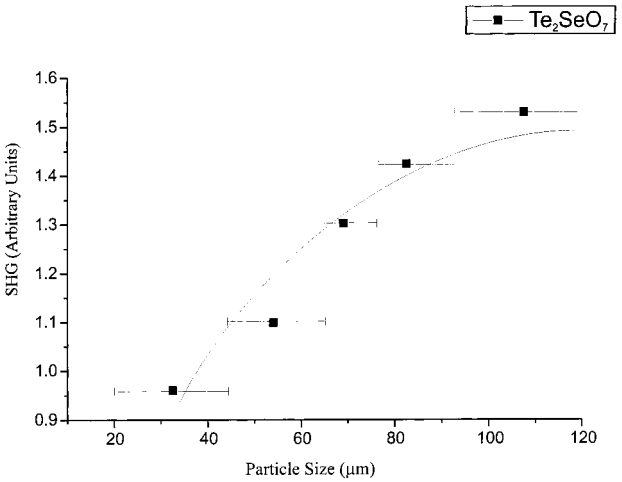

Figure 3. Phase-matching curve, i.e., particle size vs SHG intensity, for Te_2SeO_7. The curve drawn is to guide the eye and is not a fit to the data.

Second-Order NLO Measurements. *TeO_2.* The single-crystal structure[25] and NLO behavior[26] of TeO_2 have been studied in detail. However, to the best of our knowledge, no powder SHG measurements have been performed. Our measurements reveal that TeO_2 is not phase-matchable[27] (see Figure 2) and has a SHG efficiency of approximately 5 times SiO_2.

Te_2SeO_7. Powder SHG measurements indicate that Te_2SeO_7 is phase-matchable (see Figure 3) with a SHG efficiency of approximately 200 times SiO_2.

Te_2O_5. The synthesis and single-crystal structure of Te_2O_5 have been reported.[24] The researchers determined

(25) Thomas, P. A. *J. Phys. C* **1988**, *21*, 4611.
(26) Levine, B. F. *IEEE J. Quantum Electron.* **1973**, *QE-9*, 946.
(27) A formal mathematical definition of phase matching can be found in: *Handbook of Lasers*; Pressley, R. J., Ed.; CRC Press: Cleveland, 1971; pp 489−525 and references therein. Experimentally, a phase-matched material is one where the phase velocity of the fundamental frequency is equal to the phase velocity of the second-harmonic radiation. When this condition is satisfied, the frequency-doubled radiation is intensified.

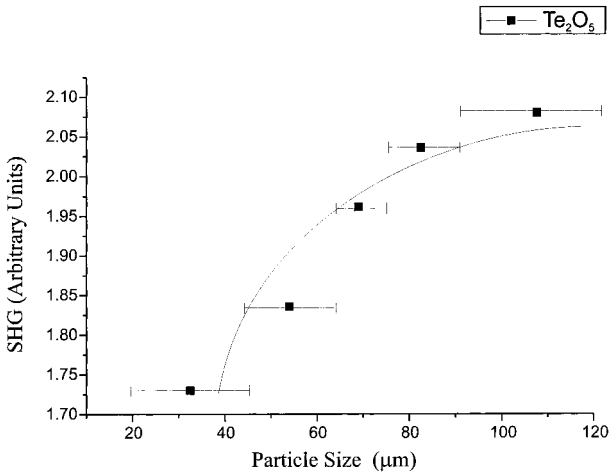

Figure 4. Phase-matching curve, i.e., particle size vs SHG intensity, for Te_2O_5. The curve drawn is to guide the eye and is not a fit to the data.

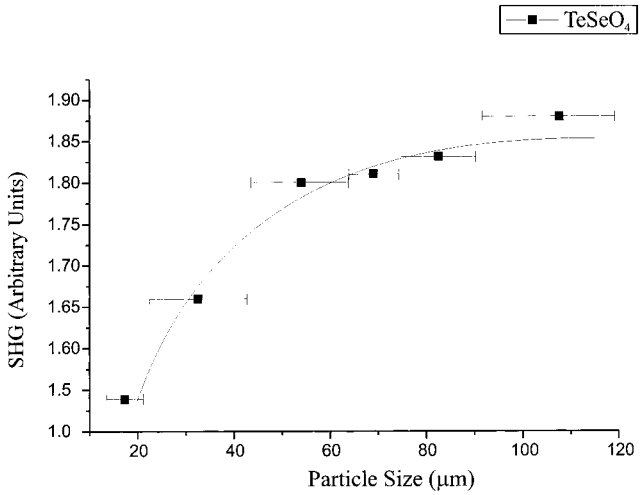

Figure 5. Phase-matching curve, i.e., particle size vs SHG intensity, for $TeSeO_4$. The curve drawn is to guide the eye and is not a fit to the data.

that the material crystallizes in the NCS space group $P2_1$ (No. 4). However, no SHG measurements were performed. Our powder SHG measurements indicate that the material is phase-matchable (see Figure 4) with a SHG efficiency of approximately 400 times SiO_2.

$TeSeO_4$. The synthesis, crystal structure, and preliminary powder SHG measurements on $TeSeO_4$ have been reported earlier.[16] More detailed measurements indicate that the material is phase-matchable (see Figure 5) with a SHG efficiency of approximately 400 times SiO_2.

Approximate NLO Susceptibilities. Typically, NLO susceptibilities, $\langle d^{2\omega}{}_{ijk}\rangle$ values, are determined from large single crystals (ca. 5 mm), usually through the Maker fringe technique.[28] The material in question must not only be grown as large single crystals but also be cut and polished, exposing specific faces. Because of the experimental difficulty of the technique and the paucity of large single crystals, individual d_{ijk} values have been determined for only a handful of the known SHG materials.

An alternative method involves powder SHG measurements that permit the approximation of the $\langle d^{2\omega}{}_{ijk}\rangle$ value for a particular material.

It has been shown earlier that for unpolarized fundamental and SHG radiation[18]

$$\langle d^{2\omega}{}_{ijk}\rangle^2 = (19/105)\sum_i d_{iii}{}^2 + (13/105)\sum_{i\neq j} d_{iii}d_{ijj} + (44/105)\sum_j d_{iij}{}^2 + (13/105)\sum_{ijk,\text{cyclic}} d_{iij}d_{jkk} + (5/7)d_{ijk}{}^2 \quad (1)$$

For quartz, in point group 32, $\langle d^{2\omega}{}_{ijk}\rangle^2 = (50/105)d_{111}{}^2$, where $d_{111} = 0.4$ pm/V,[29,30] resulting in $\langle d^{2\omega}{}_{ijk}\rangle^2 = 7.62 \times 10^{-2}$ pm^2/V^2.

The intensity of the SHG responses, for phase-matchable (PM) and non-phase-matchable (NPM) powder, are given by[18]

$$I^{2\omega}(\text{NPM}) = \langle d^{2\omega}{}_{ijk}\rangle^2 l_c{}^2/2r \quad (2)$$

with $l_c \equiv$ coherence length and $r \equiv$ average particle size, and by

$$I^{2\omega}(\text{PM}) = \langle d^{2\omega}{}_{ijk}\rangle^2[(\pi^2/4)\Gamma_{pm}] \quad (3)$$

with $\Gamma_{pm} \equiv$ average coherence length, where $\Gamma_{pm} \ll r$.

The intensity ratio for two NPM materials is

$$I^{2\omega}(\text{A})/I^{2\omega}(\text{B}) = (\langle d_A{}^{2\omega}{}_{ijk}\rangle^2 l_c{}^2/2r)/(\langle d_B{}^{2\omega}{}_{ijk}\rangle^2 l_c{}^2/2r) \quad (4)$$

For SiO_2, $l_c \approx 20$ μm and $r = 50$ μm, whereas for all of the other NPM materials, l_c and r are assumed to be 10 and 50 μm, respectively.[18]

From single-crystal data, it has been determined that $d_{14}(TeO_2) = 6.9d_{11}(SiO_2)$.[26] From our powder SHG measurements, we find that $I^{2\omega}(TeO_2)/I^{2\omega}(SiO_2) = 5$.

Setting eq 4 equal to 5, with phase A $\equiv TeO_2$ and phase B $\equiv SiO_2$, and solving for $\langle d_{TeO_2}{}^{2\omega}{}_{ijk}\rangle^2$ result in a value of 1.52 pm^2/V^2. The ratio $(\langle d_{TeO_2}{}^{2\omega}{}_{ijk}\rangle^2/\langle d_{SiO_2}{}^{2\omega}{}_{ijk}\rangle^2)^{1/2} = 4.5$, which is in reasonable agreement with the single-crystal value of 6.9.

As previously stated, powder SHG measurements on Te_2SeO_7, Te_2O_5, and $TeSeO_4$ revealed doubling efficiencies of 200, 400, and 400 times SiO_2, respectively. In addition, all three materials are also phase-matchable (see Figures 3−5). The intensity ratio for two PM materials is

$$I^{2\omega}(\text{A})/I^{2\omega}(\text{B}) = \langle d_A{}^{2\omega}{}_{ijk}\rangle^2[(\pi^2/4)\Gamma_{pm}]/\langle d_B{}^{2\omega}{}_{ijk}\rangle^2[(\pi^2/4)\Gamma_{pm}] \quad (5)$$

If Γ_{pm} is taken to be equal to 5 μm,[18] eq 5 reduces to

$$I^{2\omega}(\text{A})/I^{2\omega}(\text{B}) = \langle d_A{}^{2\omega}{}_{ijk}\rangle^2/\langle d_B{}^{2\omega}{}_{ijk}\rangle^2 \quad (6)$$

We chose $LiNbO_3$, a phase-matchable SHG material, for phase B. SHG active $LiNbO_3$ crystallizes in crystal class 3m. From eq 1[18]

(28) Maker, P. D.; Terhune, R. W.; Nisenoff, M.; Savage, C. M. *Phys. Rev. Lett.* **1962**, *8*, 21.
(29) Miller, R. C. *Appl. Phys. Lett.* **1964**, *5*, 17.
(30) Jerphagnon, J.; Kurtz, S. K. *Phys. Rev.* **1970**, *1B*, 1738.

Table 2. $I^{2\omega}$ and $\langle d^{2\omega}_{ijk}\rangle$ Values

compound	$I^{2\omega}/I^{2\omega}(SiO_2)$	$\langle d^{2\omega}_{ijk}\rangle$ (pm/V)
SiO_2	1	0.28[a]
TeO_2	5	2.47[a]
Te_2SeO_7	200	16.2[b]
Te_2O_5	400	23.1[b]
$TeSeO_4$	400	23.1[b]
$LiNbO_3$	600	28.2[a]

[a] Calculated from reported single-crystal NLO data. [b] This work.

$$\langle d^{2\omega}_{ijk}\rangle^2 = (19/105)d_{333}{}^2 + (26/105)d_{333}d_{311} + (114/105)d_{113}{}^2 + (10/21)d_{222}{}^2 \quad (7)$$

where $d_{333} = 43.75$ pm/V, $d_{311} = d_{113} = 15.38$ pm/V, and $d_{222} = 7.88$ pm/V.[30] Putting these values in eq 7 results in $\langle d_{LiNbO_3}{}^{2\omega}{}_{ijk}\rangle^2 = 7.98 \times 10^2$ pm^2/V^2. For Te_2SeO_7, Te_2O_5, and $TeSeO_4$, our powder SHG measurements indicate

$$I^{2\omega}(Te_2SeO_7)/I^{2\omega}(LiNbO_3) = 0.33$$

$$I^{2\omega}(Te_2O_5)/I^{2\omega}(LiNbO_3) = 0.67$$

$$I^{2\omega}(TeSeO_4)/I^{2\omega}(LiNbO_3) = 0.67$$

Putting these values and 7.98×10^2 pm^2/V^2 into eq 6 results in

$$\langle d_{Te_2SeO_7}{}^{2\omega}{}_{ijk}\rangle = 16.2 \text{ pm/V}$$

$$\langle d_{Te_2O_5}{}^{2\omega}{}_{ijk}\rangle = 23.1 \text{ pm/V}$$

$$\langle d_{TeSeO_4}{}^{2\omega}{}_{ijk}\rangle = 23.1 \text{ pm/V}$$

Unlike with SiO_2 and TeO_2, it is not possible to calculate *specific* d_{ijk} values because Te_2SeO_7, Te_2O_5, and $TeSeO_4$ are found in crystal classes with several independent nonzero SHG moduli. Table 2 summarizes $I^{2\omega}/I^{2\omega}(SiO_2)$ and $\langle d^{2\omega}_{ijk}\rangle$ values for the materials discussed in this paper.

Discussion

The four materials described in this paper represent a family of compounds that can provide insight into structure−SHG relationships. The materials range from a Te^{4+} complex, TeO_2, to a Te^{4+}−Se^{6+} compound, Te_2SeO_7, to a Te^{4+}−Te^{6+} mixed valent system, Te_2O_5, and finally to a Te^{4+}−Se^{4+} material, $TeSeO_4$. The powder measurements indicate SHG intensities consistent with $TeO_2 < Te_2SeO_7 < Te_2O_5 \approx TeSeO_4$. Why the materials possess specific SHG efficiencies can be understood by examining their structures.

TeO_2. The weak SHG response generated by TeO_2 can be understood structurally, as well as mathematically. TeO_2 can be described as a three-dimensional structure of linked $[TeO_{4/2}]^0$ groups. The Te^{4+} cations are in a distorted trigonal-pyramidal environment, owing to the stereoactive lone pair. The stereoactive lone pair for TeO_2 points *approximately* in the [1, 1, 0], [−1, 1, 0], [1, −1, 0], and [−1, −1, 0] directions; there is a small component of the lone pair in the *z* direction. The result is that the sum of the lone-pair polarizations is nearly zero, resulting in a weak SHG response. To understand the weak SHG efficiency of TeO_2 mathematically, one must examine the NLO bond susceptibility matrix. TeO_2 crystallizes in space group $P4_12_12$ (No. 92) that is in crystal class 422. The SHG moduli for this crystal class are given in terms of the d_{ij} NLO susceptibility matrix:[6]

$$\begin{pmatrix} 0 & 0 & 0 & d_{14} & 0 & 0 \\ 0 & 0 & 0 & 0 & -d_{14} & 0 \\ 0 & 0 & 0 & 0 & 0 & 0 \end{pmatrix}$$

where d_{14} represents the contracted notation for the matrix elements d_{123} and d_{132}. In this contracted form, Kleinman symmetry is assumed to be valid,[31] i.e., $d_{123} = d_{132}$. This assumption would result in the matrix having a value of exactly zero, and any material crystallizing in crystal class 422 should have a null SHG response. Thus, mathematically, the small SHG response from TeO_2 can be attributed to a violation of Kleinman symmetry, i.e., $d_{123} \neq d_{132}$.[26]

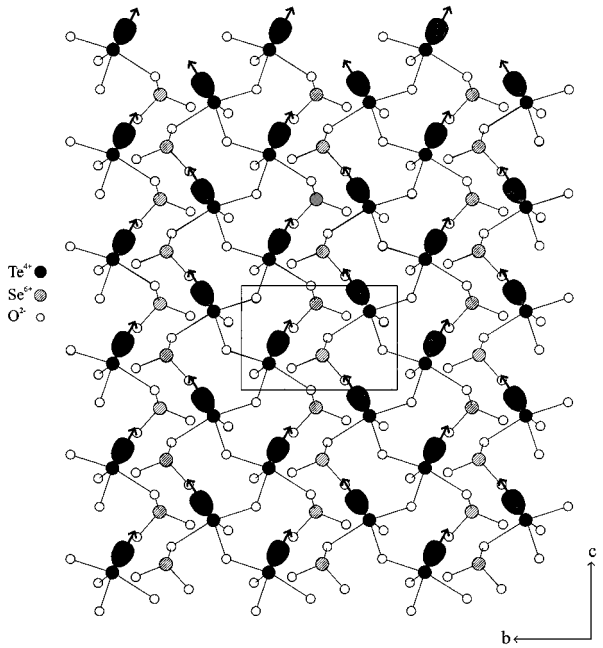

Figure 6. Ball-and-stick representation of Te_2SeO_7 with the nonbonded electron pair and dipole moment shown schematically. Note that atomic coordinates and symmetry information were taken from Te_2SO_7.[21−23]

Te_2SeO_7. With Te_2SeO_7 both Te^{4+} and Se^{6+} are observed. Se^{6+} is in a symmetric environment, and its contribution to the SHG is assumed to be negligible. As with TeO_2, the magnitude and direction of the electron pair directly influence the net polarization of the material and, consequently, the SHG behavior. Figure 6 is a ball-and-stick diagram of Te_2SeO_7 where the nonbonded electron pair and the approximate direction of the dipole moment are shown schematically. The dipole moment on each TeO_4 group is tilted, approximately 30° in the (0, 1, 1) and (0, −1, 1) planes with respect to the *c* axis. When these moments are taken as a whole, a net polarization occurs along the [0, 0, 1] plane (see Figure 6).

Te_2O_5. With Te_2O_5, both $Te^{4+}$and Te^{6+} are observed. Similar to Te_2SeO_7, we will assume no SHG contribution

(31) Kleinman, D. A. *Phys. Rev.* **1962**, *126*, 1977.

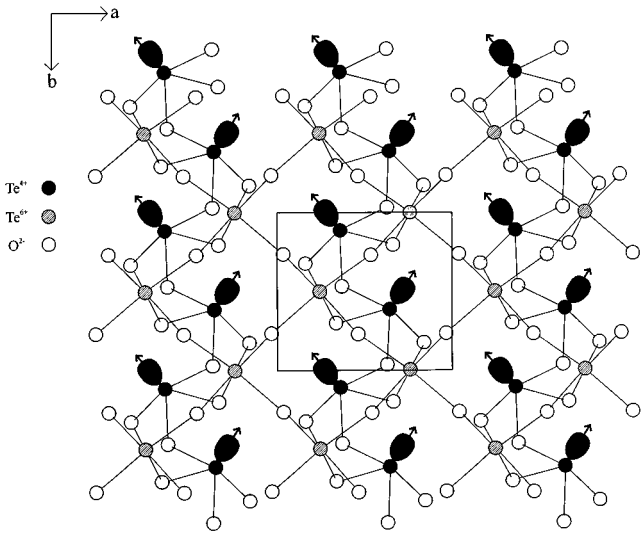

Figure 7. Ball-and-stick representation of Te_2O_5 with the nonbonded electron pair and dipole moment shown schematically.

from the regular Te^{6+} octahedra. As seen in Figure 7, the lone-pair polarization on Te^{4+} points approximately 35° into the (−1, −1, 0) and (1, −1, 0) planes, resulting in a net polarization along the [0, −1, 0] direction.

$TeSeO_4$. As previously published,[16] $TeSeO_4$ has a net lone-pair polarization in the [1, 0, 0] direction (see Figure 8).

For Te_2SeO_7, Te_2O_5, and $TeSeO_4$, it is the constructive addition of the lone-pair polarizations that results in the large SHG responses, whereas for TeO_2, it is the converse; i.e., the lone-pair polarizations nearly cancel, which produces a weak SHG signal. All of the materials that have a significant SHG response, Te_2SeO_7, Te_2O_5, and $TeSeO_4$, crystallize in polar space groups, $Pna2_1$, $P2_1$, and Ia, respectively. In addition, the direction of the net lone-pair polarization for each material is consistent with the polar axis of the respective space groups. It should be pointed out however, that a polar space group is *not* a symmetry requirement for SHG. In fact, compounds are known, e.g., $ON(CH_2)_2$ (urea), that crystallize in a NCS nonpolar space group, in this case $P-42m$, and have a significant SHG response, ~400 times SiO_2. What is important is for the individual atomic polarizations to constructively add in order to generate a significant SHG response.

Conclusions

Powder SHG experiments provide an excellent method from which to semiquantitatively measure the doubling efficiency of any material, as well as determine any phase-matching capabilities. In addition, by comparing the SHG efficiency of new materials with known compounds, one can calculate approximate NLO susceptibility values. For the materials described in this paper, we determined that the SHG efficiencies are consistent with $TeO_2 < Te_2SeO_7 < Te_2O_5 \approx TeSeO_4$, with TeO_2, Te_2SeO_7, Te_2O_5, and $TeSeO_4$ having SHG efficiencies of 5, 200, 400, and 400 times SiO_2, respectively. The variation in the SHG efficiency can be understood by taking into account the net polarization of the nonbonded electron pair. Although all of the materials crystallize in NCS space groups, only Te_2SeO_7, Te_2O_5, and $TeSeO_4$ have large SHG responses. Thus, not only is it vital for a SHG material to crystallize in a NCS space group but equally important are the atomic, or molecular, polarizations that must "constructively add" to generate a large SHG response. We are in the process of investigating the SHG properties of other NCS Te^{4+} compounds as well as Sb^{3+} complexes and will be reporting on them shortly.

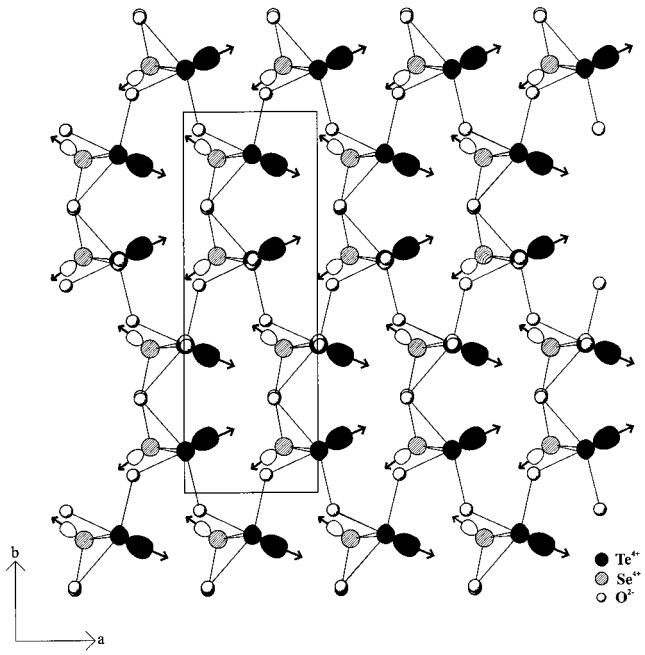

Figure 8. Ball-and-stick representation of $TeSeO_4$ with the nonbonded electron pair and dipole moment shown schematically.

Acknowledgment. We thank the Robert A. Welch Foundation for support. This work used the MRSEC/TCSUH Shared Experimental Facilities supported by the National Science Foundation under Award No. DMR-9632667 and the Texas Center for Superconductivity at the University of Houston. This work was also supported by the NSF Career Program through DMR-0092054.

CM001414U